TECHNICAL ARTICLE

Simple Fabrication and Characterization of a Platinum Microhotplate Based on Suspended Membrane Structure

F. Samaeifar[1], A. Afifi[1], and H. Abdollahi[2]

1 Department of Electrical Engineering, Malek Ashtar University of Technology, Tehran, Iran
2 Department of Electrical Engineering, Shahid Sattari Aeronautical University of Science and Technology, Tehran, Iran

Keywords
Bulk Micromachining, Microhotplate, Microsensor, MEMS, Suspended Membrane, Platinum Thin Film

Correspondence
F. Samaeifar,
Malek Ashtar University of Technology,
Tehran
Iran
Email: fsamaeifar@yahoo.com

Received: May 22, 2014;
accepted: July 22, 2014

doi:10.1007/s40799-016-0076-y

Abstract

One of the key components of a microsensor is the Micro electromechanical system (MEMS) microheater. It has a wide range of applications such as gas sensors, pressure sensors, and so on. In this study, a platinum microhotplate based on suspended membrane structure is introduced. A simple microfabrication process is adopted to form the micromachined suspended microheater. Some integrated circuit processes such as E-beam evaporation of Pt and Au, oxidation, wet etching process, and photolithography process are used to fabricate the device. As the usage of deep-reactive ion etching and low-pressure chemical vapor deposition systems are avoided, the microfabrication process of the hotplate is accessible even in laboratories with limited equipment. In order to achieve uniform temperature distribution over the active heater area and to increase the robustness of the membrane, a thin silicon island was placed underneath the dielectric membrane. Thermal and thermomechanical behaviors of this structure obtained by finite element analysis show that the designed microhotplate is relatively strong. Experimental results show that power consumption and time constant are 50 mW and 4.23 ms, respectively, for the temperature variation from 30°C to 500°C in the fabricated microhotplates.

Introduction

In recent years, thin-film microhotplates have been emerging as a topic of considerable interest for a wide variety of applications, such as gas sensors, flow/wind sensors, humidity sensors, infrared sources, and so on.[1–5] The use of microhotplate in sensor design can increase the dynamic response and significantly reduce the power consumption of the sensor due to the small thermal mass of the microhotplate.[6] Its usage as sensors can also reduce the complexity of manufacturing process[7] and the costs involved in mass production.[8]

To satisfy the needs of modern and portable electronic system applications, microhotplates are expected to have high thermal uniformity to increase the sensitivity and the selectivity of the heated layers to specific gases, low-power consumption for portable applications, high thermal and mechanical strength to intensify robustness in harsh environments, and especially compatibility with standard integrated circuit (IC) processes to enable co-integrated microsystems and to allow low-cost batch production. Finally, the ability to reach temperatures up to 700°C is an asset to perform the on-chip annealing of the deposited gas-sensitive layers after packaging.[9]

Several studies have been conducted on microheaters using Pt,[4,10–14] polysilicon,[15] and doped silicon as the heating electrode. Polyimide,[16] Si,[4,14] and SOI[17] have also been investigated for use as membrane materials. Pt is a well-known standard material for high-temperature heaters. It is electrically and thermally stable for high-temperature operation and easily available for the deposition process. It is also highly conductive and, thus, can be used with a low-drive voltage. Doped silicon- or polysilicon-based heating electrode known to be gradually degraded by silicon oxidation at high-temperature operation in ambient air, so that they require special device packaging such as inert gas sealing.[18,19]

As mentioned earlier, for gas sensors, high thermal uniformity is also critical to increase the sensitivity and selectivity to gases. As reported in Ref. 20, the temperature gradient over the sensitive area should not exceed 50°C to maintain good sensitivity performance. Briand groups recommend a temperature gradient lower than 25°C.[21] Temperature uniformity on a microhotplate can be achieved through several methods, such as using a thicker silicon island underneath the microhotplate membrane,[21,22] placing a polysilicon plate under the microhotplate membrane,[23] placing metal or a metalloid compound on the top of the heater, and using various geometries on the dielectric membrane and heater design.[24]

Despite there are numerous published literature contains the microfabrication process of microhotplate using bulk micromachining technology, they used deep-reactive ion etching (DRIE) systems[17] or deposited silicon nitrides as silicon mask during etching of Si in potassium hydroxide (KOH) using low-pressure chemical vapor deposition (LPCVD) systems[10] both of which (DIRE and LPCVD systems) are not accessible in laboratories with limited equipment. In addition, they need a vacuum chamber and the other costly instruments associated with them.

In this work, a suspended microhotplate is presented on silicon substrate with Pt heating electrode. For achieving uniform temperature distribution over the active heater area and increasing the robustness of the membrane, thin Si island is placed underneath the dielectric membrane. Simulation results using (ANSYS software, Cecil Township, Pennsylvania, USA) show that the designed microhotplate is comparability strong. In accordance with the principle of structural design, the simple fabrication processes are designed for the microhotplate. Some IC processes such as electron-beam evaporation of Pt and Au, wet etching process, and photolithography process are used to fabricate the device. For silicon bulk micromachining, a simple wet-releasing process is performed using tetramethyl ammonium hydroxide (TMAH) as Si etchant and silicon dioxide as protector of silicon during wet etching of Si in TMAH. TMAH is non-toxic to humans, no damage to integrated circuits, and compatible with CMOS technology. In addition, while using TMAH to etch silicon, thermal oxidation of silicon dioxide can be a good mask. Finally, suspended microhotplates are fabricated and characterized.

Design and Simulations

The desired structure in this article consists of a heater/thermometer element that is freely suspended via tethers. Figure 1 shows the layout of the platinum microhotplate. A rectangular island at the center is linked to the bulk silicon with four tethers. Two interdigit serpentine platinum resistors are placed in the rectangular island, and two platinum resistors enable several operational configurations. For instance, one of them is used as a heater, and the other resistor is used as a thermometer or both resistors can be used as heaters.

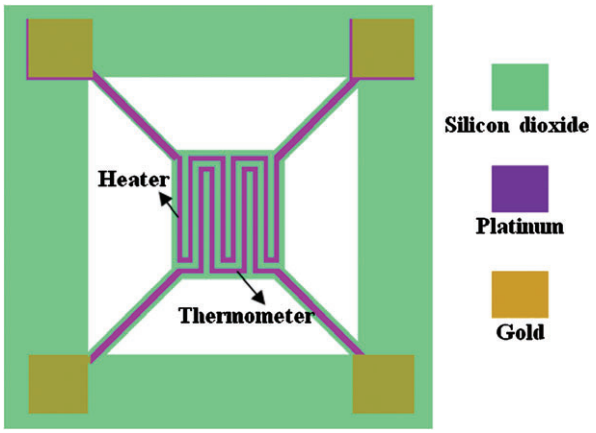

Figure 1 Schematic diagram of the top view of the microhotplate.

The designed microhotplate has been supported using thermal and mechanical simulations with the ANSYS finite element analysis software. Temperature gradient simulations and mechanical stress simulations of the structure are required to establish the geometrical features of the microhotplate. For the simulation, the ambient temperature, the applied voltage to the microhotplate, and the thermal convection coefficient are set up at 25°C, 0.35 V, and 100 W/m^2 K, respectively. It should be noted that only convective energy losses have been taken into account as the irradiative energy losses are very small due to the small the size of microhotplates and the temperature range of favorite.[25] The thermal and mechanical properties of the materials used in the microhotplate design are shown in Table 1.[23] In addition, details of the hotplate dimensions used in Finite element method (FEM) simulation are shown in Table 2.

Figure 2 shows the temperature simulation results of two microhotplates with and without silicon island underneath the dielectric membrane to compare their temperature uniformity.

For gas sensors, high thermal uniformity is critical to increase the sensitivity and selectivity to gases. Temperature uniformity on a microhotplate can be achieved through several methods. In this study,

Table 1 Material properties used for microhotplate structure[23]

Material	Density (kg μm^{-3})	Specific heat (pJ kg^{-1} K)	Thermal conductivity (pW/μm k)	Electrical conductivity (ps/μm)	Young's Modulus (Mpa)	Poisson's ratio
Si	2.33e−15	7.12e+14	1.5e8	1.44e9	1.5e5	0.17
SiO_2	2.27e−15	1.0e+15	1.4e+6	–	0.7e+5	0.2
Pt	2.14e−14	1.33e+14	7.2e+7	9.6e+12	1.68e+5	0.38
Au	1.93e−14	1.29e+14	2.97e+8	45.2e+12	7.8e+4	0.44

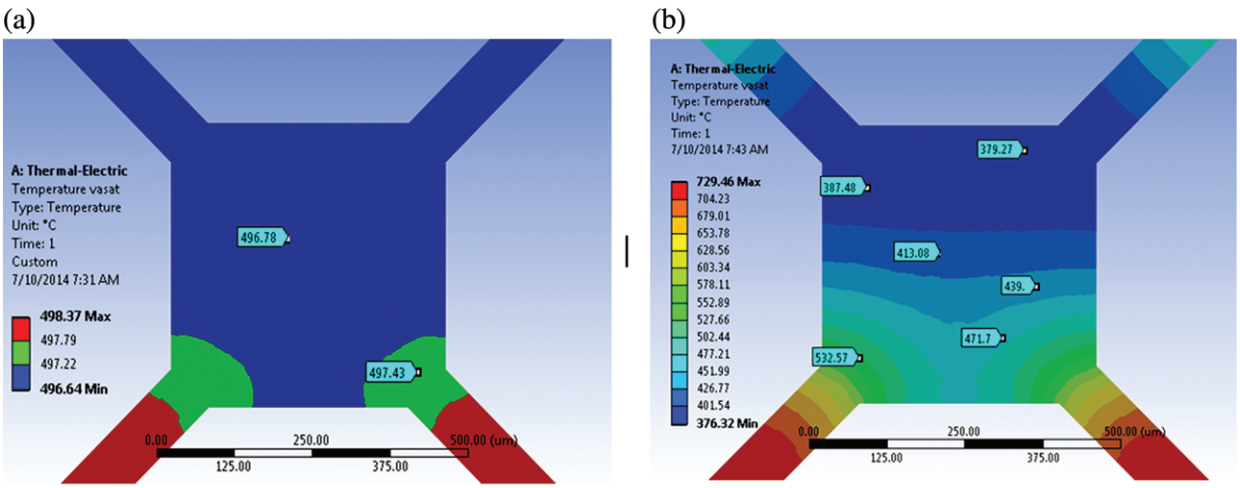

Figure 2 Microheater (a) with and (b) without a silicon island under the dielectric membrane.

Table 2 Dimensions of the microhotplate

Structure	Dimension (μm)
Membrane length	1000
Heater length	440
Heater width	20
Tether length	400
Tether width	50
Silicon thickness	10
Silicon dioxide thickness	0.3
Platinum thickness	0.12
Gold thickness	0.15

the method of placing silicon island underneath the dielectric membrane is investigated. As it is shown in Fig. 2, the microhotplate with silicon island has high temperature uniformity in heater-active area, whereas the microhotplate without silicon island has high temperature gradient (more than 80°C) in its active area. Therefore, we chose suspended membrane microhotplate with silicon island underneath the active area in our structure.

Simulation results of the mechanical stress and the vertical displacement of the microhotplate at 500°C using ANSYS software are shown in Figs. 3 and 4, respectively. The mechanical stress is on the order of 100–170 MPa which is less than the compressive strength of silicon dioxide (about 690 MPa) and the vertical displacement is about 3 μm for the suspended microhotplate. These results show that the designed microhotplate is relatively strong.

Device Fabrication

Fabrication of the suspended membrane microhotplate involves five photolithographic processes with four masks carried out using optical lithography and standard cleanroom processes. The microfabrication process typically consists of 13 steps: growing of the silicon oxide layer on the substrate, evaporation of the chromium film in the front side, patterning of back-side silicon oxide layer, etching of silicon, patterning the front-side chromium layer, repeating the silicon etching, removing of silicon oxide layer, removing chromium layer, growing a new silicon oxide on the substrate, patterning of front-side silicon oxide layer, evaporation of Cr, Pt, and Au

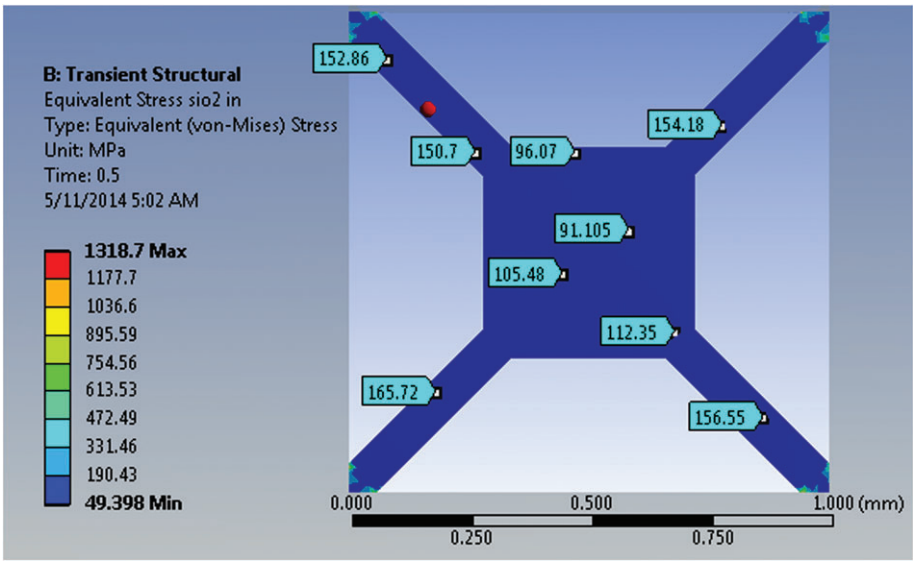

Figure 3 FEM simulation of the mechanical stress in the microhotplate.

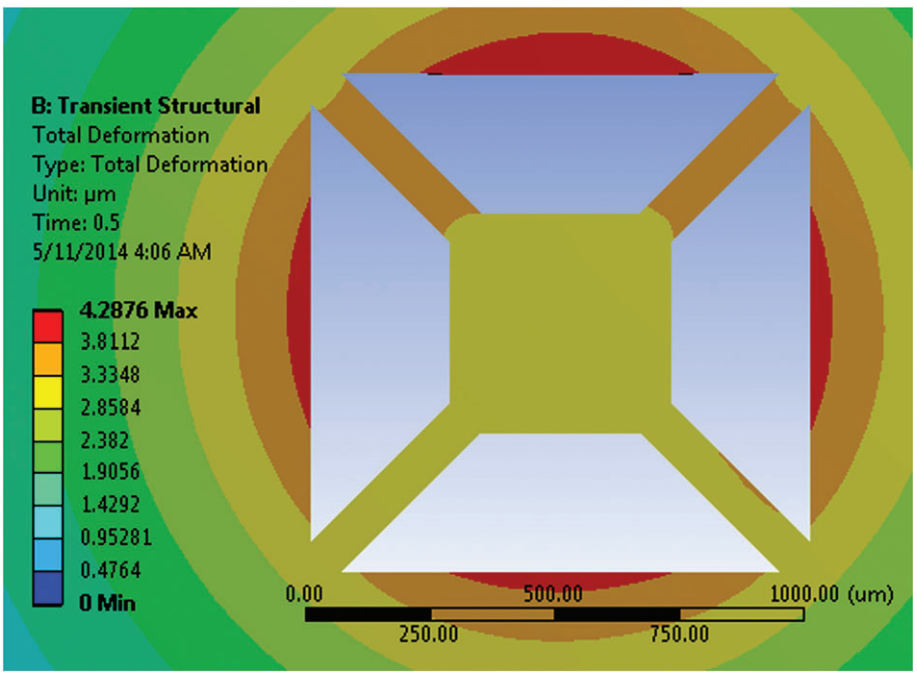

Figure 4 FEM simulation of the vertical displacement in the microhotplate.

respectively on front side and patterned by liftoff process, etching the front-side silicon, and releasing of the structure.

Figure 5 shows the basic fabrication steps used to implement the simple fabrication microhotplate in this work.

The micromachined structure was fabricated on a p-type ‹100› Si wafer with the thickness of 460 µm. The wafer is cleaned by Radio Corporation of America (RCA) cleaning process. First, a 1-µm-thick SiO_2 is thermally grown on double-side polished substrate by means of wet oxidation process (Fig. 5(a)), then 150 nm thick Cr layer is then evaporated on top of the SiO_2 on the front side of wafer using thermal evaporation method (Fig. 5(b)). This Cr layer is used for SiO_2 patterning and extra protection of SiO_2 during the subsequence etching of Si in TMAH. Cr deposition is followed by 1 h annealing at 400°C at 5 sccm nitrogen flow pressure. After that, a square window is opened on the back side of SiO_2 using standard lithography process by buffered hydrofluoric acid (BOE) etchant (Fig. 5(c)). Subsequently, the silicon substrate is etched using commercially available TMAH (25%; Merk, Hohenbrunn, Germany)

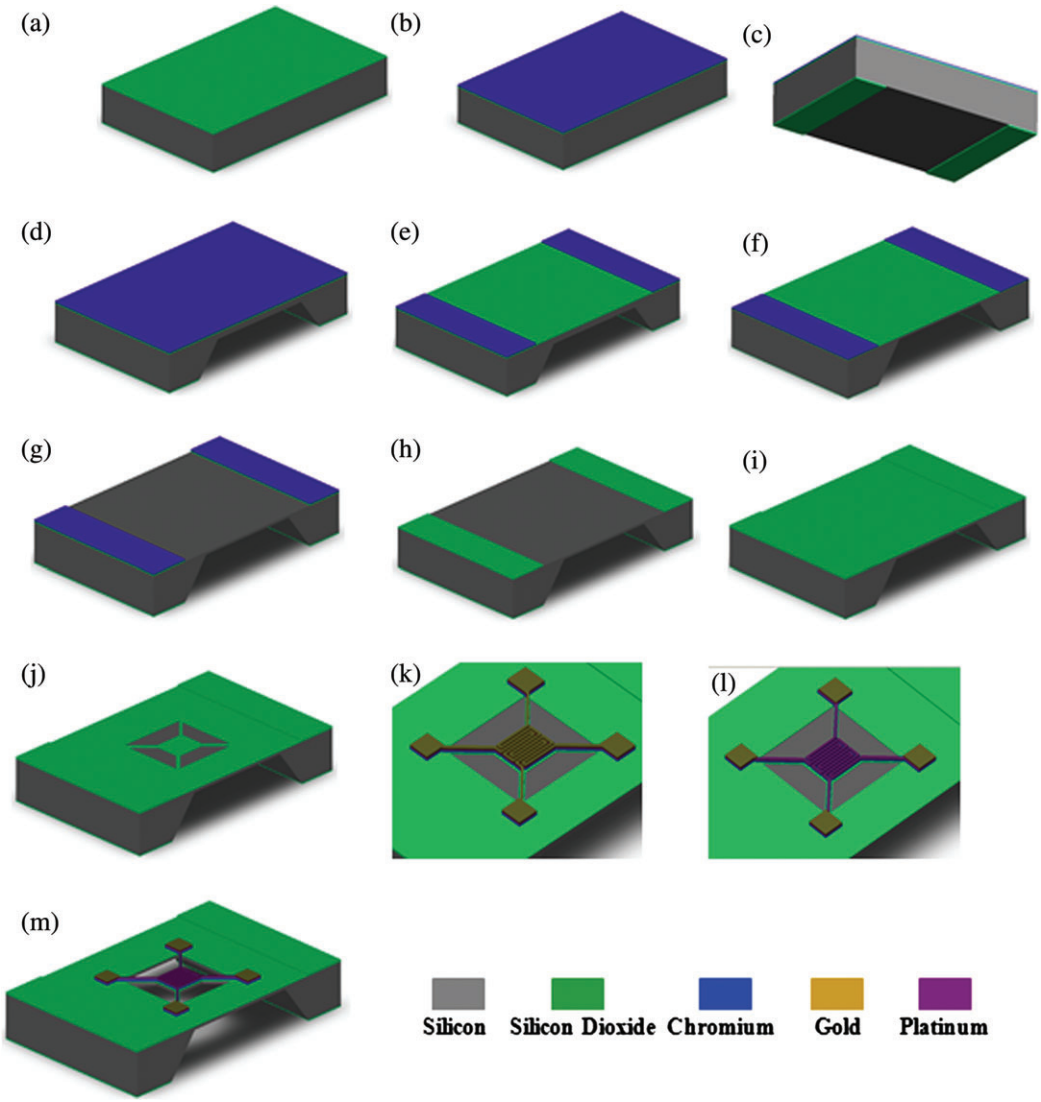

Figure 5 Fabrication process of the microhotplate: (a) growing of the 1-μm-thick SiO_2 mask layer on the substrate, (b) evaporation of the 150-nm-thick Cr mask layer on the SiO_2 in the front side, (c) patterning of back-side SiO_2 layer by BOE etchant, (d) etching of Si using TMAH etchant to make 60-μm-thin membrane, (e) double-sided lithography used to pattern in the front-side Cr layer, (f) continuing the silicon etching again to observe red thin film membrane, (g) removing of SiO_2 layer using BOE etchant, (h) removing Cr layer completely, (i) growing 300-nm-thick SiO_2 layer on front side, (j) patterning of front-side SiO_2 layer, (k) evaporation of Ti, Pt, and Au films respectively on front side and patterned by liftoff process, (l) patterning of Au layer, and (m) release of the structure.

at 90°C for 6 h to make 60-μm-thin membranes (Fig. 5(d)).[26] Double-sided lithography is used to pattern the front-side and back-side square windows. Cr is then etched by Ammonium Cerium (IV) Nitrate ($(NH_4)_2Ce(NO_3)_6$) diluted with deionized water for 30 s (Fig. 5(e)).

Back-side silicon substrate etching is again continued by immersion in TMAH (25 %) until red thin film membrane is observed (Fig. 5(f)). The SiO_2 layer is then removed completely using BOE for 20 min (Fig. 5(g)). This process is practiced because the previously grown SiO_2 had lost its quality during different thermal and chemical process. Following this step, Cr is removed completely by Cr etchant using aqueous $(NH_4)_2Ce(NO_3)_6$ for 30 s (Fig. 5(h)). A fresh 300-nm thick SiO_2 layer is then thermally grown on front-side substrate (Fig. 5(i)). The SiO_2 structure is then patterned on the front side of silicon substrate with photolithography technique using wet etching technique by BOE etchant (Fig. 5(j)). After that, the wafers are spin-coated with positive photoresist on the fronts and patterned, then Ti, Pt, and Au are

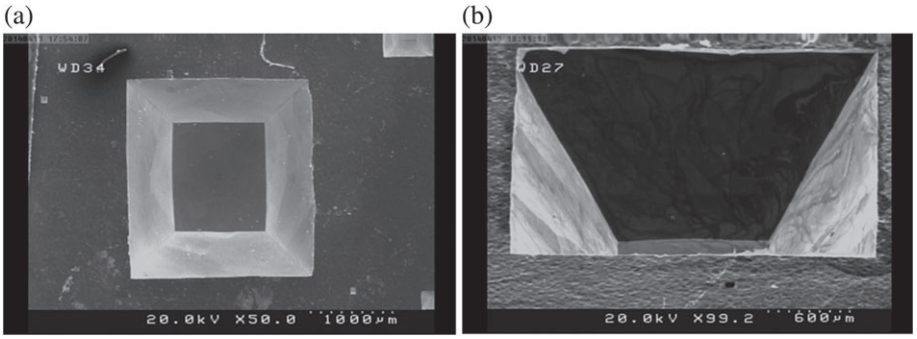

Figure 6 SEM image of (a) top view and (b) cross-sectional view of the back-side membrane.

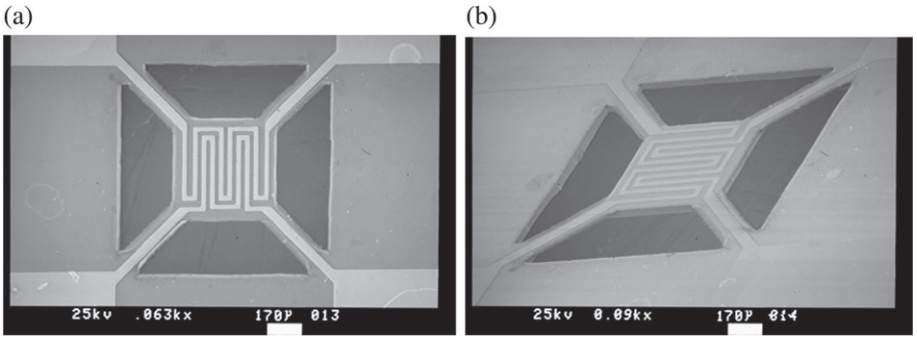

Figure 7 SEM image of (a) top view and (b) cross-sectional view of the fabricated microhotplate.

deposited by e-beam evaporation one by one with the thickness of 20, 120, and 150 nm, respectively. A lift-off technique is used to form Ti–Pt–Au trimetallic wires (Fig. 5(k)). Subsequently, Au is patterned and etched (in a saturated solution of KI in H_2O and 1 iodine crystal) (Fig. 5(l)). Finally, the front-side silicon is etched using 25% TMAH at $T = 90^{\circ}C$, and the structures are released (Fig.5(m)). Figure 6(a) and (b) shows SEM images of top and cross-sectional view of the back-side etching using TMAH etching process. A smooth bottom of the crater indicates the successful etching of the silicon without hillock formation. Figure 7(a) and (b) shows SEM images of the top and cross-sectional view of the fabricated microhotplate, respectively.

Results and Discussion

The fabricated microhotplates consist of two platinum resistors each of which can be used as either a heater or a resistive thermometer. We used one of the resistors as a heater and another resistor as a thermometer, and studied the temperature characteristics of the heater element, the power consumption, and the time constants of the device. To calculate the temperature coefficient resistance

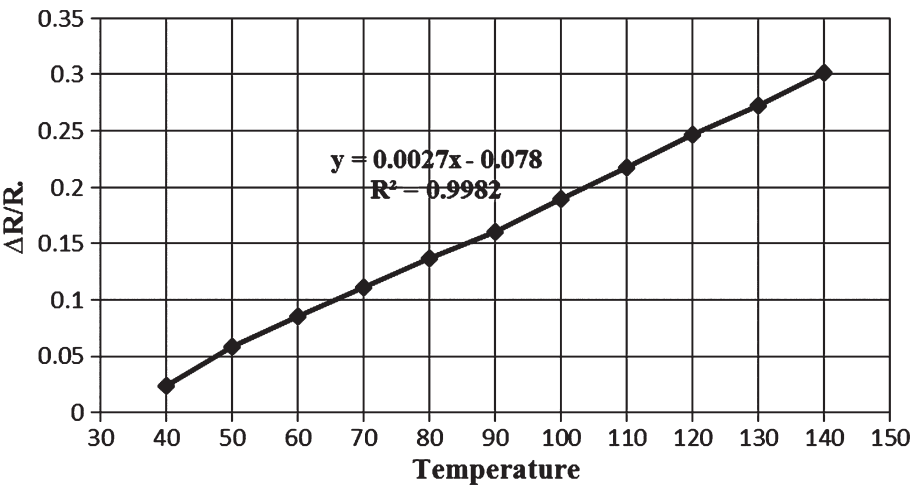

Figure 8 Calibration curve obtained using a temperature controlled system. The resulting slope yields a TCR value of $2.7 \times 10^{-3}\ C^{-1}$.

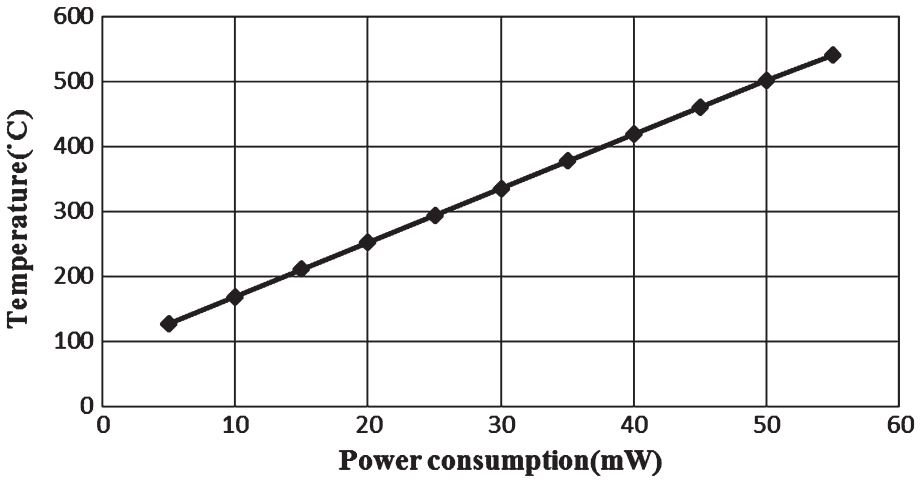

Figure 9 Variation of the temperature of the microhotplate as a function of the power consumption of the device.

characteristic of the platinum heater, a calibration curve has been obtained. For that, the device was placed into an oven with a temperature reference sensor and the change in resistance was measured for different temperature steps as shown in Fig. 8. The temperature response proves linear and a TCR value of $2.7 \times 10^{-3}\,C^{-1}$ was calculated. This value of the TCR is in good agreement with the reported literature for a platinum-based element. However, it is lower than the theoretical value of bulk platinum ($3.9 \times 10^{-3}\,C^{-3}$). This is possibly due to the electron scattering at grain boundary in films.[27]

In Fig. 9, the heater temperature as a function of heater power consumption of the device is presented. As it is shown in this figure, the temperature as high as 500°C can be reached by applying 50 mW power.

The response time of the microhotplate (i.e. the time needed for the microhotplate to reach 63% of its final steady-state temperature) has also been measured. To measure the response time, a current pulse was applied on the heater and the signal of thermometer was obtained by using the thermometer connected in Wheatstone bridge circuits.

The transient response of the temperature has also been measured. To measure the response time, a current pulse was applied on the heater. A dedicated circuit was used to transform a typical voltage pulse into a current pulse (Fig. 10).

Figure 11 shows voltage of the thermometer as a function of time when the square current pulse of 5 mA with 70 ms duration is applied to the heater. As shown this picture which is plotted directly from the measured instrument, heating time constant is 4.23 in the temperature range of room temperature up to 500°C.

The microhotplate achieves high heating efficiency and short response time that is comparable

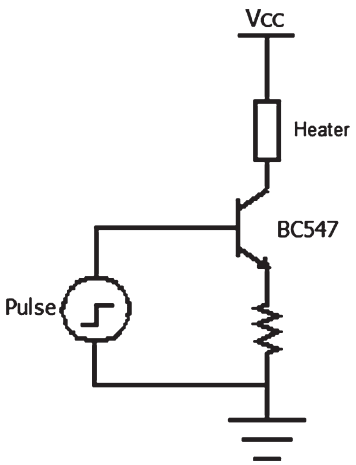

Figure 10 Voltage of the current pulse generator used to extract the response time of the device.

or superior to previously published platinum microhotplate.[4,10–14] In addition, better temperature uniformity is expected in the heater due to the relatively high thermal conductivity of silicon.

Conclusion

In this study, a suspended microhotplate using silicon substrate and platinum as the heating electrode material has been designed, fabricated, and characterized. Simulation using ANSYS software showed that microhotplate with silicon island underneath the dielectric membrane has high temperature uniformity. Moreover, the simulation results of mechanical stress and the vertical displacement of the microhotplate show that the designed microhotplate is relatively strong. Simple fabrication processes were designed in which TMAH is used as silicon etchant and silicon dioxide

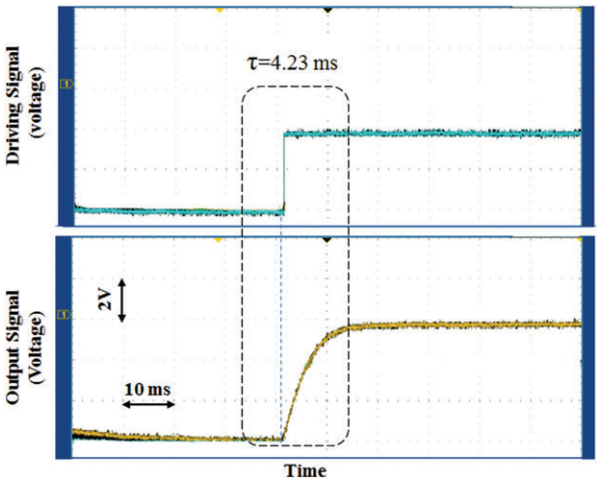

Figure 11 Voltage of the thermometer as a function of time when a square current pulse is applied to heater.

is used as protector of silicon during etching of Si in TMAH. Measured electrical and thermal behaviors of the fabricated microhotplate show that the power consumption and the response time of the microhotplate are better than those of most platinum-based microhotplates that were previously reported. Moreover, the robustness and temperature uniformity are improved due to the relatively high thermal conductivity of silicon island underneath the microhotplate membrane.

Reference

1. Courbat, J., Canonica, M., Teyssieux, D., Briand, D., and De Rooij, N., ''Design and Fabrication of Micro-hotplates Made on a Polyimide Foil: Electrothermal Simulation and Characterization to Achieve Power Consumption in the Low mW Range,'' *Journal of Micromechanics and Microengineering* **21**: 015014 (2010).
2. Dai, C.-L., ''A Capacitive Humidity Sensor Integrated with Micro Heater and Ring Oscillator Circuit Fabricated by CMOS–MEMS Technique,'' *Sensors and Actuators B: Chemical* **122**: 375–380 (2007).
3. Elmi, I., Zampolli, S., Cozzani, E., Mancarella, F., and Cardinali, G., ''Development of ultra-low-power consumption MOX sensors with ppb-level VOC detection capabilities for emerging applications,'' *Sensors and Actuators B: Chemical* **135**: 342–351 (2008).
4. Hwang, W.-J., Shin, K.-S., Roh, J.-H., Lee, D.-S., and Choa, S.-H., ''Development of micro-heaters with optimized temperature compensation design for gas sensors,'' *Sensors* **11**: 2580–2591 (2011).
5. Konz, W., Hildenbrand, J., Bauersfeld, M., et al., ''Micromachined IR-source with Excellent Blackbody Like Behaviour,'' *Proceedings of SPIE* **5836**: 540–548 (2005).
6. Tao, C., Yin, C., He, M., and Tu, S., ''Thermal Analysis and Design of a Micro-hotplate for Si-substrated Micro-structural Gas Sensor,'' *3rd IEEE International Conference on Nano/Micro Engineered and Molecular Systems (NEMS 2008), Sanya*, Hainan Island, China, pp. 284–287 (2008).
7. Courbat, J., Briand, D., and De Rooij, N.F., ''Reliability Improvement of Suspended Platinum-based Micro-heating Elements,'' *Sensors and Actuators A: Physical* **142**: 284–291 (2008).
8. Chung, G.-S., and Jeong, J.-M., ''Fabrication of Micro Heaters on Polycrystalline 3C-SiC Suspended Membranes for Gas Sensors and their Characteristics,'' *Microelectronic Engineering* **87**: 2348–2352 (2010).
9. Laconte, J., Flandre, D., and Raskin, J.-P., *Micromachined Thin-film Sensors for SOI-CMOS Co-integration*, Volume **XIII**, *Springer*, Berlin, Germany, p. 292 (2006ISBN: 0-387-28842-2).
10. Belmonte, J.C., Puigcorbe, J., Arbiol, J., et al., ''High-Temperature Low-power Performing Micromachined Suspended Micro-hotplate for Gas Sensing Applications,'' *Sensors and Actuators B: Chemical* **114**: 826–835 (2006).
11. Guo, B., Bermak, A., Chan, P.C., and Yan, G.-Z., ''A Monolithic Integrated 4× 4 Tin Oxide Gas Sensor Array with On-Chip Multiplexing and Differential Readout Circuits,'' *Solid-State Electronics* **51**: 69–76 (2007).
12. Hotovy, I., Rehacek, V., Mika, F., et al., ''Gallium Arsenide Suspended Microheater for MEMS Sensor Arrays,'' *Microsystem Technologies* **14**: 629–635 (2008).
13. Lee, D.-S., Shim, C.-H., Lim, J.-W., Huh, J.-S., Lee, D.-D., and Kim, Y.-T., ''A Microsensor Array with Porous Tin Oxide Thin Films and Microhotplate Dangled by Wires in Air,'' *Sensors and Actuators B: Chemical* **83**: 250–255 (2002).
14. Lee, K.-N., Lee, D.-S., Jung, S.-W., Jang, Y.-H., Kim, Y.-K., and Seong, W.-K., ''A High-temperature MEMS Heater Using Suspended Silicon Structures,'' *Journal of Micromechanics and Microengineering* **19**: 115011 (2009).
15. Ehmann, M., Ruther, P., von Arx, M., and Paul, O., ''Operation and Short-term Drift of Polysilicon-heated CMOS Microstructures at Temperatures up to 1200 K,'' *Journal of Micromechanics and Microengineering* **11**: 397 (2001).
16. Aslam, M., Gregory, C., and Hatfield, J., ''Polyimide Membrane for Micro-heated Gas Sensor Array,''

Sensors and Actuators B: Chemical **103**: 153–157 (2004).
17. Yi, X., Lai, J., Liang, H., and Zhai, X., ''Fabrication of a MEMS Micro-hotplate,'' *Journal of Physics: Conference Series* **276**: 012098 (2011).
18. Bauer, D., Heeger, M., Gebhard, M., and Benecke, W., ''Design and Fabrication of a Thermal Infrared Emitter,'' *Sensors and Actuators A: Physical* **55**: 57–63 (1996).
19. Kishi, N., and Hara, H., ''Lifetime Evaluation of Self-modulated MEMS Infrared Light Source Made of Single Crystalline Silicon,'' *SICE, 2007 Annual Conference, Kagawa University*, Takamatsu City, Kagawa, Japan, pp. 2451–2454 (2007).
20. Astié, S., Gue, A., Scheid, E., and Guillemet, J., ''Design of a Low Power SnO_2 Gas Sensor Integrated on Silicon Oxynitride Membrane,'' *Sensors and Actuators B: Chemical* **67**: 84–88 (2000).
21. Briand, D., Gretillat, M., and van der Schoot, B., and De Rooij, N., ''Thermal Management of Micro-hotplates Using MEMCAD as Simulation Tool,'' *Proceedings of the MSM 2000 International Conference On Modeling and Simulation of Microsystems, U.S. Grant hotel*, San Diego, March 27–29 (2000).
22. Ruther, P., Ehmann, M., Lindemann, T., and Paul, O., ''Dependence of the Temperature Distribution in Micro Hotplates on Heater Geometry and Heating Mode,'' *12th International Conference on Transducers, Solid-State Sensors, Actuators and Microsystems*, Boston, MA, pp. 73–76 (2003).
23. Dennis, J.O., Ahmed, A.Y., and Mohamad, N.M., ''Design, Simulation and Modeling of a Micromachined High Temperature Microhotplate for Application in Trace Gas Detection,'' *International Journal of Engineering and Technology* **10**: 89–96 (2010).
24. Sidek, O., Ishak, M., Khalid, M., Abu Bakar, M., and Miskam, M., ''Effect of Heater Geometry on the High Temperature Distribution on a MEMS micro-hotplate,'' *2011 3rd Asia Symposium on Quality Electronic Design (ASQED)*, Kuala Lumpur, Malaysia, pp. 100–104 (2011).
25. Lee, J., Spadaccini, C.M., Mukerjee, E.V., and King, W.P., ''Differential Scanning Calorimeter Based on Suspended Membrane Single Crystal Silicon Microhotplate,'' *Journal of Microelectromechanical Systems* **17**: 1513–1525 (2008).
26. Abdollahi H, Hajghassem H, Mohajerzadeh S. Simple Fabrication of an Uncooled Al/SiO_2 Microcantilever IR Detector Based on Bulk Micromachining. *Microsystem Technologies* **20**: 387–396 (2014).
27. Mayadas, A., and Shatzkes, M., ''Electrical-resistivity Model for Polycrystalline Films: The Case of Arbitrary Reflection at External Surfaces,'' *Physical Review B* **1**: 1382 (1970).